



This is a repository copy of *Genomic landscape of hepatocellular carcinoma in Egyptian patients by whole exome sequencing*.

White Rose Research Online URL for this paper:

<https://eprints.whiterose.ac.uk/216026/>

Version: Published Version

Article:

Kassem, P.H., Montasser, I.F., Mahmoud, R.M. et al. (13 more authors) (2024) Genomic landscape of hepatocellular carcinoma in Egyptian patients by whole exome sequencing. BMC Medical Genomics, 17. 202.

<https://doi.org/10.1186/s12920-024-01965-w>

Reuse

This article is distributed under the terms of the Creative Commons Attribution-NonCommercial-NoDerivs (CC BY-NC-ND) licence. This licence only allows you to download this work and share it with others as long as you credit the authors, but you can't change the article in any way or use it commercially. More information and the full terms of the licence here: <https://creativecommons.org/licenses/>

Takedown

If you consider content in White Rose Research Online to be in breach of UK law, please notify us by emailing eprints@whiterose.ac.uk including the URL of the record and the reason for the withdrawal request.



eprints@whiterose.ac.uk
<https://eprints.whiterose.ac.uk/>

RESEARCH

Open Access



Genomic landscape of hepatocellular carcinoma in Egyptian patients by whole exome sequencing

Perihan Hamdy Kassem¹, Iman Fawzy Montasser^{2*}, Ramy Mohamed Mahmoud¹, Rasha Ahmed Ghorab¹, Dina A. AbdelHakam¹, Marium EL Sayed Ahmad Fathi¹, Marwa A. Abdel Wahed¹, Khaled Mohey¹, Mariam Ibrahim⁴, Mohamed El Hadidi^{5,6}, Yasmine M. Massoud², Manar Salah², Arwa Abugable⁷, Mohamad Bahaa³, Sherif El Khamisy⁷ and Mahmoud El Meteini³

Abstract

Background Hepatocellular carcinoma (HCC) is the most common primary liver cancer. Chronic hepatitis and liver cirrhosis lead to accumulation of genetic alterations driving HCC pathogenesis. This study is designed to explore genomic landscape of HCC in Egyptian patients by whole exome sequencing.

Methods Whole exome sequencing using Ion Torrent was done on 13 HCC patients, who underwent surgical intervention (7 patients underwent living donor liver transplantation (LDLT) and 6 patients had surgical resection).

Results Mutational signature was mostly S1, S5, S6, and S12 in HCC. Analysis of highly mutated genes in both HCC and Non-HCC revealed the presence of highly mutated genes in HCC (*AHNAK2*, *MUC6*, *MUC16*, *TTN*, *ZNF17*, *FLG*, *MUC12*, *OBSCN*, *PDE4DIP*, *MUC5b*, and *HYDIN*). Among the 26 significantly mutated HCC genes—identified across 10 genome sequencing studies—in addition to TCGA, *APOB* and *RP1L1* showed the highest number of mutations in both HCC and Non-HCC tissues. Tier 1, Tier 2 variants in TCGA SMGs in HCC and Non-HCC (*TP53*, *PIK3CA*, *CDKN2A*, and *BAP1*). Cancer Genome Landscape analysis revealed Tier 1 and Tier 2 variants in HCC (*MSH2*) and in Non-HCC (*KMT2D* and *ATM*). For KEGG analysis, the significantly annotated clusters in HCC were Notch signaling, Wnt signaling, PI3K-AKT pathway, Hippo signaling, Apelin signaling, Hedgehog (Hh) signaling, and MAPK signaling, in addition to ECM-receptor interaction, focal adhesion, and calcium signaling. Tier 1 and Tier 2 variants *KIT*, *KMT2D*, *NOTCH1*, *KMT2C*, *PIK3CA*, *KIT*, *SMARCA4*, *ATM*, *PTEN*, *MSH2*, and *PTCH1* were low frequency variants in both HCC and Non-HCC.

Conclusion Our results are in accordance with previous studies in HCC regarding highly mutated genes, TCGA and specifically enriched pathways in HCC. Analysis for clinical interpretation of variants revealed the presence of Tier 1 and Tier 2 variants that represent potential clinically actionable targets. The use of sequencing techniques to detect structural variants and novel techniques as single cell sequencing together with multiomics transcriptomics, metagenomics will integrate the molecular pathogenesis of HCC in Egyptian patients.

Keywords Hepatocellular carcinoma (HCC), Living Donor Liver Transplantation (LDLT), Whole exome sequencing, Mutational signature

*Correspondence:

Iman Fawzy Montasser
imanfawzy2@gmail.com

Full list of author information is available at the end of the article



© The Author(s) 2024. **Open Access** This article is licensed under a Creative Commons Attribution-NonCommercial-NoDerivatives 4.0 International License, which permits any non-commercial use, sharing, distribution and reproduction in any medium or format, as long as you give appropriate credit to the original author(s) and the source, provide a link to the Creative Commons licence, and indicate if you modified the licensed material. You do not have permission under this licence to share adapted material derived from this article or parts of it. The images or other third party material in this article are included in the article's Creative Commons licence, unless indicated otherwise in a credit line to the material. If material is not included in the article's Creative Commons licence and your intended use is not permitted by statutory regulation or exceeds the permitted use, you will need to obtain permission directly from the copyright holder. To view a copy of this licence, visit <http://creativecommons.org/licenses/by-nc-nd/4.0/>.

Introduction

Hepatocellular carcinoma (HCC) is the most common primary liver cancer, ranking the third leading cause of cancer related mortalities [1]. Chronic hepatitis and liver cirrhosis lead to accumulation of genetic alterations driving HCC pathogenesis. In Egypt, HCC constitutes a significant public health problem, where it is responsible for 33.63% and 13.54% of all cancers in males and females, respectively. There is a strong link between HCC and the hepatitis C virus (HCV) epidemic affecting 10–15% of the Egyptian population, which is reported as the highest prevalence of HCV in the world [2]. The molecular mechanisms driving HCC tumorigenesis are extremely complex and an understanding of these driver mutations is essential for prevention, as well as diagnostic, prognostic, and therapeutic purposes [3, 4]. However, these key genetic drivers remain unstudied, and an understanding of the underlying molecular mechanisms process in the development of HCC in Egyptian population is necessary, of which this study adds to relevance.

According to the European Association for Study of the Liver (EASL) guidelines, one of the unmet needs in HCC research is to develop new tools for early detection including the assessment of liquid biopsy (blood sample) [5]. In addition, without a liver biopsy, assessment of the genomic profile can be addressed by a noninvasive liquid biopsy which provides actionable genomic information without the risk of complications. Using a liquid biopsy, ctDNA can be extracted to comprehensively profile the tumor genome better than conventional sampling methods [6, 7].

Hepatocellular carcinoma is highly heterogeneous malignancy and recent studies found that HCC commonly presents with mutations in the TERT promoter, *TP53*, *CTNNB1*, *AXIN1*, *LAMA2*, *ARID1A*, *WWP1*, and *RPS6KA3* genes. Somatic mutations that are HCC-associated vary extensively among individuals and even within a single tumor [8]. Among the causes of genomic intratumor heterogeneity (ITH) including somatic mutations, epigenetic changes, and large-scale genomic alterations, somatic alterations represent the most abundant and studied mutations among cancers. Interplay between mutated driver genes is a major determinant of the carcinogenic process [9].

Several studies have attempted to identify driver mutations within the protein coding regions or the exomes in various types of cancers. Although the exomes represent 1% of human genome, it covers 85% of the disease-causing mutations. For this reason, sequencing of the whole exome using whole exome sequencing (WES) has the potential to discover a large number of variants implicated in many diseases including cancers [10].

The widespread use of next-generation sequencing (NGS) offers in-depth investigation into the tumor type-specific and context-driven characteristics of ITH. Next generation sequencing using WES enables researchers to create the precise genomic profile of HCC and identify protein-altering mutations per tumor in relation to clinicopathologic criteria [11]. It provides a detailed understanding of cancer pathways and the discovery of molecular mechanisms of cancer. It can throw light on the frequent somatic/genetic alterations in driver genes and the main pathways dysregulated in HCC [12, 13].

Ethnicity could contribute to global differences in the molecular profile of HCC due to the presence of various risk factors such as hepatitis B virus, hepatitis C virus, alcohol, aflatoxin exposure and metabolic syndrome [10]. Consequently, in our study we performed WES on dual HCC and surrounding non-HCC tissue samples for each HCC patient. To overview somatic mutations in the form of single nucleotide polymorphisms (SNPs) and assess their clinical relevance in HCC patients, we analyzed the type and number of SNPs in each gene and the association between them and clinicopathological information. In addition, we analyzed the pathways affected and the agreement with previous results in other populations in international databases on HCC. We analyzed the common variants between all studied patients and the presence of novel mutations aiming to generate a genomic profile for HCC Egyptian patients.

Subjects and methods

The subjects of this prospective study were Egyptian patients with HCC attending Ain Shams Centre for Organ Transplantation (ASCOT), and Hepato-pancreatico-biliary unit (HPB) Ain Shams University Hospitals, Cairo, Egypt, between October 2020 and June 2022. Our study was approved by the Faculty of Medicine Ain Shams University Research Ethics Committee (FMASU R92/2020).

Subjects

Sixteen patients underwent surgical intervention (7 patients had surgical resection and 9 patients underwent living donor liver transplantation (LDLT)). Patients were subjected to genomic profiling using whole exome sequencing.

All transplanted patients were HCC on top of HCV cirrhosis, out of 7 patients who underwent resection, 4 patients were HCV-HCC, 2 patients were HBV-HCC and 1 patient had Budd-Chiari syndrome.

Criteria for Liver transplantation selection for HCC patients ($n=9$):

- 1) Age from 18–65 years.

- 2) Milan Criteria ($n=6$), (single lesion greater ≥ 2 cm and ≤ 5 cm, or up to 3 lesions, ≥ 1 cm and less than or ≤ 3 cm) [14]
- 3) UCSF criteria ($n=1$), (single tumor ≤ 6.5 cm or ≤ 3 tumors with the largest tumor diameter ≤ 4.5 cm and total tumor diameter ≤ 8 cm) [15]
- 4) Patients beyond UCSF are selected as case by case study after successful down staging and radiological criteria showing complete response (CR) or stable disease (ST) according to Modified RECIST (mRECIST) criteria [16] with no evidence of any macrovascular invasion or distant extra hepatic spread ($n=2$).
- 5) Alpha-fetoprotein ≤ 200 ng/dl.

Criteria for HCC Eligibility for Hepatic resection ($n=7$):

- 1) BCLC A (Single, or ≤ 3 nodules each ≤ 3 cm, Preserved liver function, PS 0) [17],
- 2) Intermediate stage HCC according to Hong Kong liver cancer stage [2, 18]
- 3) Child A or early B [7, 8].
- 4) No evidence of portal hypertension.
- 5) Patients unfit for or refuse liver transplantation.

Methods

Whole exome sequencing was performed using Ion Torrent (Ion Chef and Ion Proton) for sequencing of HCC and non-HCC samples from 16 Egyptian HCC patients. After explanation of the process, receiving consent and signatures from participant patients, 2 tissue samples were obtained from each HCC patients, from both HCC liver tissue and surrounding non-HCC tissue. Four patients' samples were prepared as fresh frozen paraffin embedded (FFPE) by the pathology department of Ain Shams Specialized Hospital Liver Tissue (LT) (LT2, LT6, LT7, LT8). Samples from patients LT1,3,4,5 were excluded either due to death of patient or technical problems. As a result of the observed low quality of DNA extracted from FFPE samples, as evidenced by gel electrophoresis, the following 12 patients' samples were taken as fresh tissue samples intraoperative by surgeon on a stabilizing solution for DNA named RNALater (RNALater™ Stabilization Solution, ThermoFisher) according to manufacturer instructions. Samples were processed within a max of three days preserved at 2–4 °C.

DNA Extraction

- FFPE samples: samples were fixed in 4–10% formalin as quickly as possible after surgical removal for a fixation time of 14–24 h (longer fixation times

lead to more severe DNA fragmentation, resulting in poor performance in downstream assays). As recommended by the manufacturer, samples were thoroughly dehydrated prior to embedding (residual formalin can inhibit the digestion of proteinase K). Stained sections were examined by the pathologist to ensure more than 20% cancer cells in HCC samples. DNA extraction from FFPE was done using QiaAmp DNA FFPE kit (Cat. No. / ID: 56,404, Qiagen). Starting material for DNA purification consisted of freshly cut sections of FFPE tissue, each with a thickness of up to 10 μm . Up to 8 sections, each with a thickness of up to 10 μm and a surface area of up to 250 mm^2 , can be combined in one preparation.

- Fresh samples: For fresh tissue, samples were cut to a maximum thickness of 0.5 cm and submerged in 5 volumes of RNALater as recommended by manufacturer (RNALater™ Stabilization Solution, ThermoFisher). Samples were stored at 2–4 °C for a max of 3 days until processed. Fresh tissue samples were extracted using QiaAmp DNA Mini Kit (Qiagen). 25 mg of liver tissue were used as a starting material.
- After extraction: Using Qubit dsDNA HS assay (ThermoFisher Scientific) DNA was quantitated and purity tested using NanoDrop Microvolume Spectrophotometer (ThermoFisher Scientific) (Supplement Table 1). Purity (the ratio of absorbance at 260 and 280 nm is used to assess DNA purity) was accepted for all samples (Ratio ~ 1.8) [19], with a mean concentration of 60.7 ng/uL (14.8–127.6), FFPE samples mean concentration 58.4 ng/uL (21–120), fresh samples 60 ng/uL (14.8–127.6). Sample LT15 was excluded from WES because of exceptionally low concentration and unaccepted purity value of DNA in addition to LT9, 12 due to a failure in the sequencing step.

Whole Exome Sequencing

The breakdown of steps in whole exome sequencing is shown in Table 1. Library preparation was executed using Ion AmpliSeq Exome RDY Library Preparation kit (ThermoFisher Scientific). The amount of DNA required was 50–100 ng in a volume not exceeding 56 μL . We amplified target regions from 50–100 ng of genomic DNA (gDNA) in the IonAmpliSeq™ Exome RDY plates using the 5X Ion AmpliSeq™ HiFi Mix. Target amplification reactions were combined and then amplicons partially digested with FuPa Reagent. Ligation of barcode adapters with Switch Solution and DNA Ligase followed, which then was purified. We normalized the libraries after quantification using qPCR Ion Library Taqman Quantitation Kit on Via 7

Table 1 A breakdown outline for the steps used for sequencing HCC tissue samples

No	Step	Kit	Manufacture	Instrument
1	DNA Extraction	QIAamp DNA mini Kit	Qiagen	—
2	Measure concentration of DNA (QC Step)	Qubit dsDNA HS assay	ThermoFisher Scientific	Qubit 3.0
3	Amplify the targets	Ion AmpliSeq™ Exome RDY Kit / Ion Xpress™ Barcode Adapters	ThermoFisher Scientific	9700 Thermal Cycler
4	Partially digest amplicons			
5	Ligate barcoded adapters to the amplicons			
6	Purify the unamplified library	Agencourt™ AMPure™ XP Reagent	Beckman Coulter	DynaMag™-2 Magnet
7	Quantify the library	Ion Library Taqman Quantitation Kit	ThermoFisher Scientific	Via 7 Real Time PCR
8	Template preparation, loading chips and sequencing	Ion PI™ Hi-Q™ Chef Kit	Ion Torrent	Ion Chef
9		Ion PI™ Chip		Ion Proton

Real Time PCR machine (ThermoFisher) and diluted to 100 pM. Template preparation and amplification was implemented using emulsion PCR on Ion sphere particles (ISP) and we combined two barcoded exome libraries on a single Ion 540™ Chip using Ion PI™ Hi-Q™ Chef Kit on Ion Chef system. Finally, sequencing was performed on Ion Proton™ system using semiconductor technology based on detection of hydrogen ions released during the DNA synthesis reaction by a highly sensitive pH meter—a microchip sensor.

Bioinformatics

Reads were initially demultiplexed and aligned to hg19 human reference sequence using the variantCaller v5.12.0.4 (Torrent server software—Thermo Fisher Scientific) which ran as embedded instance within Ion Torrent S5 sequencer. The resulting alignment BAMs were further processed using Ion Reporter™ Software 5.18 pipeline (Thermo Fisher Scientific), which incorporated variant calling and annotate variants based on the most updated databases such as ClinVar, DrugBank, GO, etc. The existence of potentially significant variants was further reassessed through manual inspection of aligned reads in IGV 2.4 software.

Available clinical significance annotation was assessed in real-time from Human Gene Mutation Database Professional (<https://portal.biobase-international.com/hgmd/pro/>), ClinVar (<https://www.ncbi.nlm.nih.gov/ClinVar/>) and dbSNP.

(<https://www.ncbi.nlm.nih.gov/snp>). The predictions for SIFT, PolyPhen and PhyloP tools were retrieved from the IonReporter result files (tab-separated files). Frequency data was provided by Ensembl/VEP release 108.0; additionally, gnomAD v3.1 database was queried for allele frequencies of individual variants (<http://gnomad.broadinstitute.org>).

Variant annotation

The VCF files were uploaded on the main Galaxy public server on <https://usegalaxy.org>. SnpEff eff (Galaxy Version 4.3 + T.galaxy2) was used to annotate and predict the effect of these variants [20]. The SnpEff 4.3 hg19 genome data was downloaded using SnpEff download and applied as the genome source for SnpEff eff. The default settings were selected for upstream/downstream length of 5000 base, the set size for splice sites which was set to 2 bases as well as for spliceRegion Settings. For the annotation options, the following were selected: Add loss of function (LOF) and nonsense mediated decay (NMD) tags. The chromosomal position was based on the input type and “-chr” was prepended to the chromosome name. SnpSift Extract Fields was then used on the VCF output files from SnpEff eff to extract specific fields and organize them in a tabular file [20].

Data processing

MUTALISK was aided in determination of mutational signature in HCC samples [21]. A web-based version of OpenCRAVAT (<https://run.opencravat.org>) was used for performing genomic variant interpretation including variant impact, annotation, and scoring [22]. CancerSpecific High-throughput Annotation of Somatic Mutations (CHASM) was used as well [23]. CHASM-plus discriminates somatic missense mutations as either cancer drivers or passengers. Predictions can be done in either a cancer type-specific manner or by a model considering multiple cancer types together. TARGET is a database of genes that, when somatically altered in cancer, are directly linked to a clinical action. TARGET genes may be predictive of response or resistance to a therapy, prognostic, and/or diagnostic [24]. Oncogenes and tumor suppressor genes were delineated as described by Vogelstein et al., 2013 [25]. Franklin was used to analyze variants according

to ACMG classification for somatic variants [26]. David Annotation database was used for assessment of enrichment driver pathways in our HCC samples [27].

Results

Liver tissue (HCC and non-HCC) and corresponding blood samples were collected from 16 HCC patients including 15 males (94%) and 1 female (6%), with a median age of 59 years (IQR 51–60 years). Of these, 13 patients had HCV and 2 patients had HBV (LT9, LT13), while 1 patient suffered from Budd-Chiari syndrome (LT11). According to Milan staging, 6 patients followed Milan Criteria (66.7%), 1 patient followed UCSF criteria (11.1%), and 2 patients were beyond both (22.2%). Regarding BCLC clinical staging system, 7 cases were stage A (43.7%), 6 cases were stage B (37.5%), and 3 cases were stage D (18.8%). Among the sixteen enrolled patients, tissue biopsy was taken from HCC and non-HCC liver tissue from 9 patients during liver transplantation, while 7 were sampled during hepatic resection.

Variant types

Using whole exome sequencing, the exons and surrounding noncoding genomic regions of protein-coding genes were captured in pairs of tumor and non-cancerous liver tissues. Genomic regions of variants varied from exon to non-exon variants (Supplement Table 2). Among pathogenic variants (Missense (27.9%), frameshift (1.6%), stop-gained (1.5%) and splice-site (0.4%)), missense was the highest percentage as shown in Fig. 1 and in Supplement Table 3.

Mutational signatures

We analyzed HCC samples via Mutalisk against 30 mutational signatures COSMIC v2 [21] (Fig. 2; Supplement Table 4, Supplement Table 1). Analysis showed predominance of single base substitutions S1, S5, and S23 in FFPE samples (LT2, LT6, LT7, LT8) and S1, S5, S6, and S12 in fresh tissue samples (LT10, LT11, LT13, LT14, LT16, LT17, LT18, LT19, LT20). Signature 1 is the result of an endogenous mutational process initiated by spontaneous deamination of 5-methylcytosine. The number of S1 mutations correlates with age of cancer diagnosis. Signature 5 is found in all cancer types and most cancer samples. The etiology of S5 is unknown. Signature 6 is found in many cancer types and is most common in colorectal and uterine cancers. In most other cancer types, S6 is found in less than 3% of examined samples. S6 is associated with defective DNA mismatch repair and is found in microsatellite unstable tumors, S6 is associated with high numbers of small (<3 bp) insertions and deletions at mono/polynucleotide repeats. Signatures 12 and 23 are found in liver cancer. Their etiology remains unknown [21]. Whole results are shown in Supplement MUTALISK Mutational signatures HCC.

Highly mutated genes (highest number of somatic variants)

Analysis of highly mutated genes was done using OpenCRAVAT. Genes showing the highest somatic mutations in HCC and Non-HCC are shown in Tables 2, 3. Analysis of highly mutated genes in both HCC and Non-HCC revealed the presence of 10 common highly mutated genes (AHNAK2, MUC6, MUC16, TTN, ZNF17, FLG, MUC12, OBSCN, PDE4DIP, MUC5b, and HYDIN)

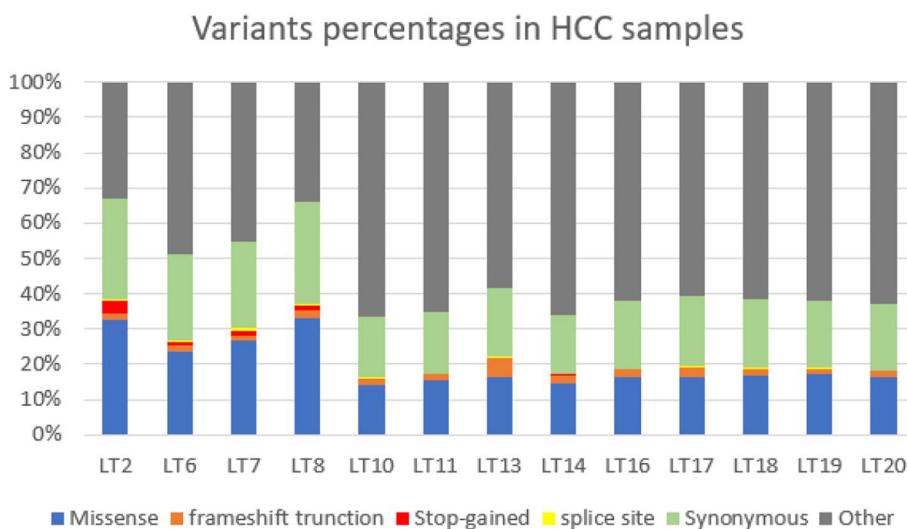


Fig. 1 Percentage of different variant sequence ontologies in HCC samples

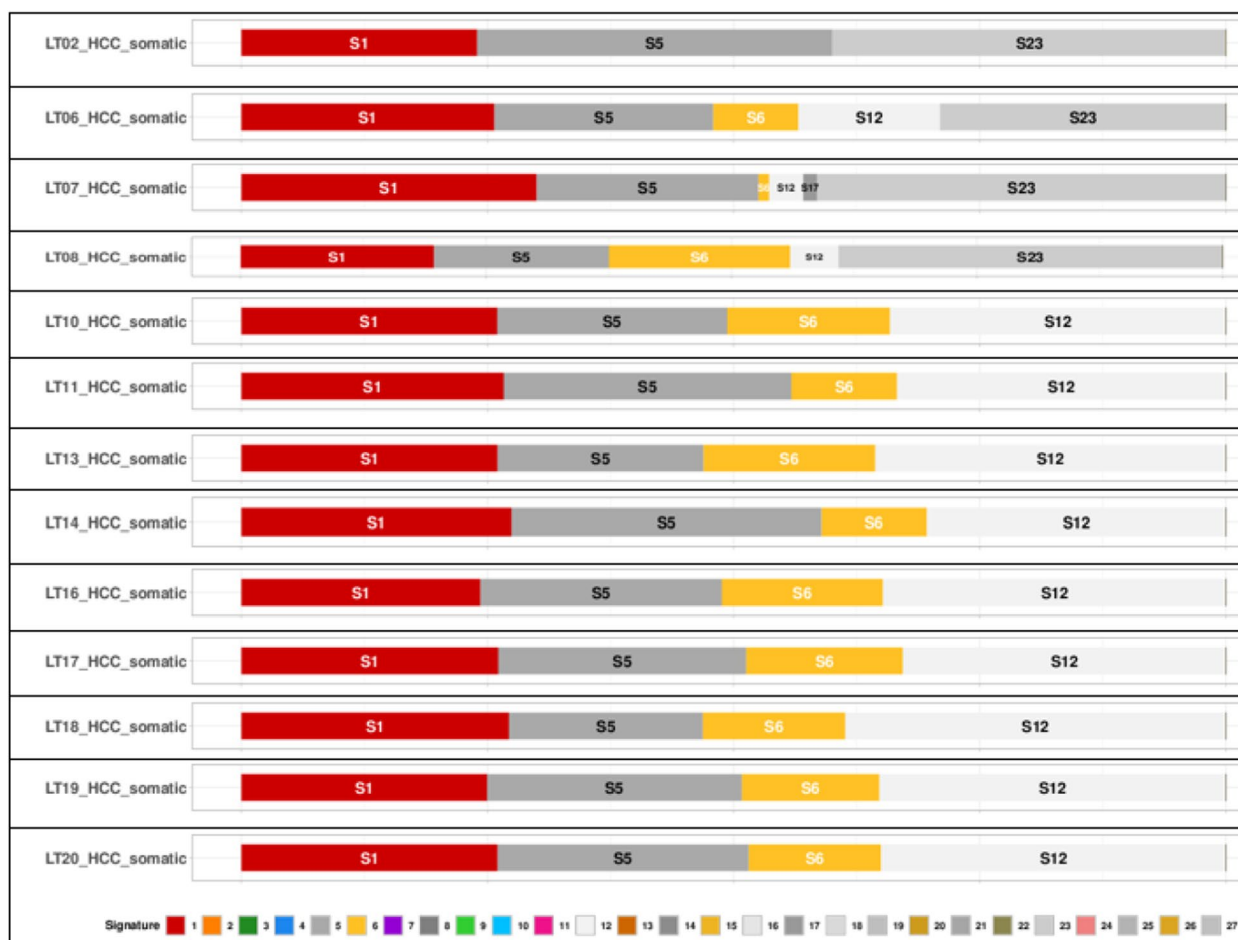


Fig. 2 Mutational signatures in HCC samples showing predominance of S1, S5 and S23 in FFPE samples (LT2, LT6, LT7, LT8) and S1, S5, S6, and S12 in fresh tissue samples (LT10, LT11, LT13, LT14, LT16, LT17, LT18, LT19, LT20) [21]

(Supplement Tables 5, 6). Mapping of variants on the most highly mutated genes (AHNAK2, MUC16, MUC6, FLG, PDE4DIP, and HYDIN) relative to The Cancer Genome Atlas in HCC (TCGA LIHC) [28, 29] is shown in Fig. 3. Comutant OBSCN and TTN are shown in HCC and Non-HCC (Table 4).

The Cancer Genome Atlas (TCGA) significantly mutated genes

The Cancer Genome Atlas (TCGA) network performed a large-scale multi-platform analysis of HCC, including evaluation of somatic mutations in 363 patients. Whole exome sequencing on 363 HCC cases revealed that 12,136 genes had non-silent mutations, and 26 significantly mutated genes (SMGs) were determined using the MutSigCV algorithm [28, 29]. The list includes the 26 significantly mutated HCC genes identified across 10 genome sequencing studies in addition to TCGA and is shown in Supplement file TCGA HCC.

We studied the somatic variants in HCC and Non-HCC tissues regarding the 26 significantly mutated genes to determine the type and number of mutations in patients’ liver tissue. Data analysis revealed the presence of 87 unique variants in HCC and 94 in non-HCC tissues, most were frameshift truncation as demonstrated in Fig. 4. Genes *APOB* and *RP1L1* showed the highest number of mutations in both HCC and Non-HCC tissues (Fig. 5). Frameshift mutations comprised 77% in HCC and 66% in Non-HCC tissues, while missense were 21% and 31%, respectively. Analysis of unique variants in individual samples revealed the presence of Tier 1, Tier 2 variants in SMGs in HCC and Non-HCC (*TP53*, *PIK3CA*, *CDKN2A*, and *BAP1*) among variants with CScape score for driver point mutation exceeding 0.5 [30] are listed in Table 5. CScape Coding predicts the oncogenic status (disease-driver or neutral) of somatic point mutations (missense in our list) specifically in the coding region of the cancer genome values above 0.5 are predicted to be deleterious, while those below 0.5 are predicted to be neutral

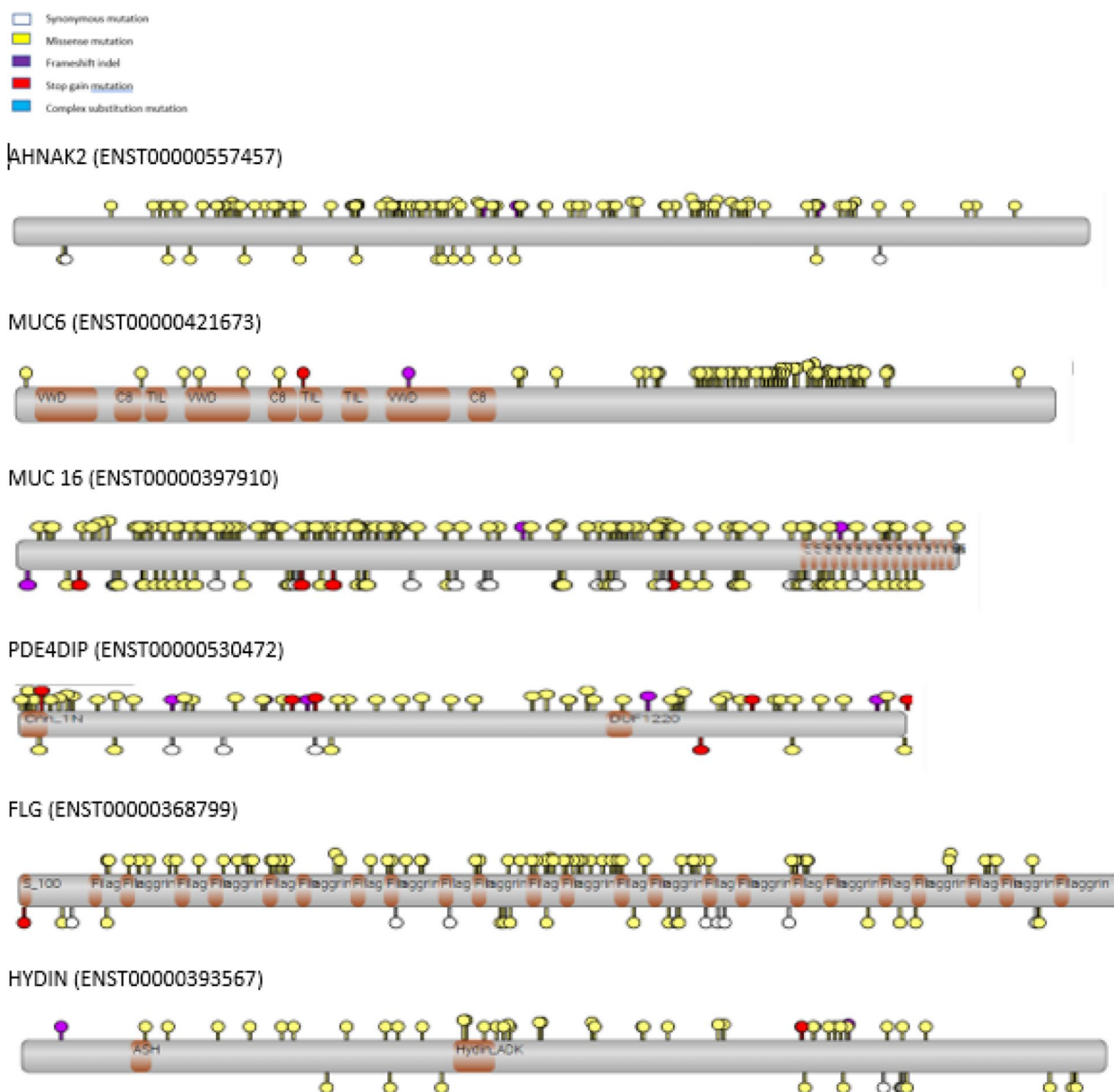


Fig. 3 Variants in highly mutated genes HCC from our study (Above the bar), and the variants from TCGA HCC (Below the bar) are shown as a lollipop diagram, Protein domains are shown as brown bars. Variants in multiple samples are taller. Color Sequence ontology of variant

or benign [30]. Only *BAP1* had 2 variants with CScore exceeding 0.5 in Non-HCC TCGA SMGs. Table 6 demonstrates the distribution of different variants in TCGA SMGs in our HCC and Non-HCC patients. A list showing the frequency of TCGA SMGs and their number among HCC and Non-HCC samples is shown in Table 6.

Cancer genome landscape

Oncogenes and tumor suppressor genes harbored pathogenic and non-pathogenic mutations. The percentage

of unique TSGs mutations were higher (63%) than unique oncogenes mutations (37%) in HCC samples. Missense (60%) were more prevalent than frameshift (37%) in both with a fewer percentage of stop gained and splice site variants, and with a higher percentage of frameshift in TSGs relative to oncogenes (Supplement Table 7). Unique pathogenic variants with a Phred score exceeding 20, missense variants were sorted according to CHASMplus LIHC (Hepatocellular carcinoma) score in HCC samples, with Tier 1 and Tier 2 variants

Table 2 Heatmap for pathogenic variants in highly mutated genes in HCC samples

Genes HCC	LT2	LT6	LT7	LT8	LT10	LT11	LT13	LT14	LT16	LT17	LT18	LT19	LT20	Grand total
AHNAK2	1	23	4	13	33	37	85	48	48	48	26	53	31	450
ZNF717				4	35	50	35	58	58	58		41	40	379
MUC6		37	15	9	31	34	56	29	29	29	7	34	35	345
MUC16		3	3		21	46	54	44	44	44	9	21	16	305
PDE4DIP		6	9	5	27	30	62	30	30	30	10	21	24	284
FLG	1	23	10	6	7	41	5	29	29	29	21	35	9	245
HYDIN		6	10	2	18	21	62	19	19	19	7	21	21	225
TTN		3	2		17	15	65	24	24	24	7	19	15	215
MUC12	1	13	9	10	25	34	27	17	17	17	1	20	19	210
OBSCN		8	25	2	14	18	19	14	14	14	9	15	13	165
MUC5B	2	6	15	2	2	15	35	7	7	7	8	10	9	125
Grand Total	5	128	102	53	230	341	505	319	319	319	105	290	232	

Table 3 Heatmap for pathogenic variants in highly mutated genes in Non-HCC samples

High mutated Non-HCC	LT6	LT7	LT8	LT10	LT11	LT13	LT14	LT16	LT18	LT19	LT20	Grand total
MUC6		5	7	47	40	41	39	46	54	39	46	364
AHNAK2		7	17	48	35	34	31	38	50	55	36	351
ZNF717				47	45			43	23	44	32	234
MUC16				42	41	9	12	36	33	15	14	202
FLG	6	17	5	11	36	1	30	2	34	32	9	183
MUC12		7	4	29	20	10	17	27	3	20	17	154
PDE4DIP		8		33	25	2	10	28	15	13	16	150
OBSCN		26	2	16	16	2	7	15	14	18	11	127
MUC17		6		7	6	31	13	6	2	5	8	84
TTN				24	10		2	10	5	13	10	74
Grand Total	6	76	35	304	274	130	161	251	233	254	199	

Table 4 Commutant OBSCN and TTN HCC and Non-HCC samples

OBSCN TTN	LT6	LT7	LT8	LT10	LT11	LT13	LT14	LT16	LT17	LT18	LT19	LT20	Total	
HCC	OBSCN	8	25	2	14	18	5	14	17	5	9	16	14	147
	TTN	3	2		19	15	28	25	22	5	7	20	15	161
Non-HCC	OBSCN		26	2	16	16	2	7	15	2	14	18	11	129
	TTN				24	10		2	10	3	5	13	10	77

(*TP53*, *CDKN2A*, and *MSH2*) according to ACMG criteria by Franklin delineated in (Fig. 5) and in Supplement Table 8 including chromosome position mapped against GRCH37, targeted treatment, Phred score and zygosity. Unique pathogenic variants with Phred score more than 20, missense variants were sorted according to CHASMplus LIHC (Hepatocellular carcinoma) score in Non-HCC samples, with Tier 1 and Tier 2 variants

(*KMT2D* and *ATM*) according to ACMG criteria by Franklin delineated in Fig. 6 and in Supplement Table 9.

Pathways in Hepatocellular carcinoma

To reveal the potential role of mutated genes in biological process, we conducted Gene Ontology (GO) and Kyoto Encyclopedia of Genes and Genomes (KEGG) annotation using David annotation tools [27] in HCC samples,

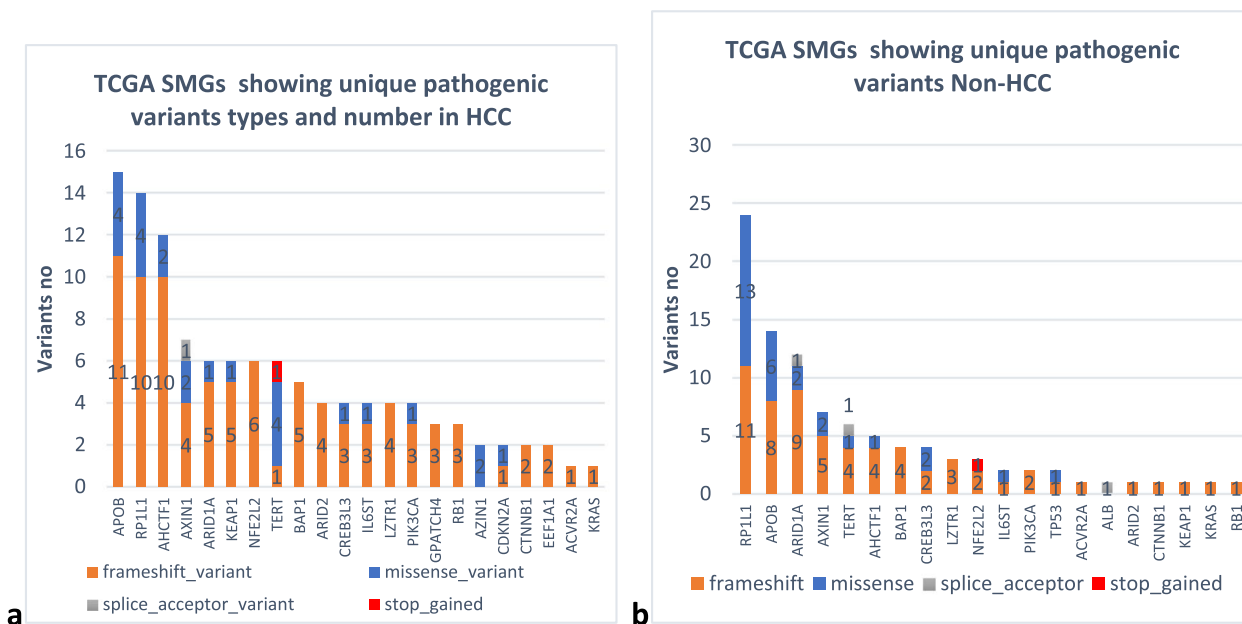


Fig. 4 Unique pathogenic variants involving TCGA SMGs in both (a) HCC and (b) Non-HCC

analysis of results is listed in Supplement file Go KEGG HCC. Results for the most significant KEGG pathways are shown in Table 7. For KEGG analysis, among the significantly annotated clusters were Notch signaling, Wnt signaling, PI3K-AKT pathway, Hippo signaling, Apelin signaling, Hedgehog (Hh) signaling, and MAPK signaling, in addition to ECM-receptor interaction, focal adhesion, and calcium signaling which are crucial landmarks in a hepatocellular carcinoma pathway. Pathogenic mutations in genes in all HCC samples, among HCC pathway, are illustrated in Supplement Fig. 2.

Tier 1 and Tier 2 variants

We performed database search on Franklin to reassess the somatic category of variants by other studies and to assess the category according to Association for Molecular Pathology (AMP) standards [26]. Eight variants proved to be (3, Tier 1 and 5, Tier 2) with a Phred score >20 (*TP53*, *CDKN2A*, and *MSH2* in individual HCC samples, *Kit* variant common in 3 HCC, *KMT2D* (3 variants in Non-HCC), and *ATM* in Non-HCC, in addition to other 15 variants with Phred score <20 (*KMT2D*, *NOTCH1*, *KMT2C*, *PIK3CA*, *KIT*, *SMARCA4*, *ATM*, *PTEN*, *MSH2*, and *PTCH1*). These variants are rare in population studies as revealed by gnomAD frequency on OpenCravat less than 0.1 (Table 8). All the previous mutations are clinically targetable with specific inhibitors. A list of 134 variants (Supplement Table 10) Tier 1 and Tier 2 low frequency variants including those before, and other variants that were low confidence.

Discussion

Currently, three types of NGS-based analytical methods are mainly used to identify genomic mutations: (i) whole exome sequencing (WES), (ii) whole-genome sequencing (WGS), and (iii) targeted sequencing (TS). This study was done to explore the mutational landscape in Egyptian patients with HCC using whole exome sequencing on both HCC and Non-HCC liver tissue.

In our study, missense was the highest prevalence, followed by synonymous variants with no significant difference between them, with frameshift and stop gained showing much lower percentages. This agrees with other cancer studies where the most called variants are commonly synonymous, followed by non-synonymous and splice site variants; however, the less common frameshift and stop gained/stop loss variants are more likely to have deleterious effects at the protein level, which guides variant prioritization. Although assumed benign and excluded, synonymous variants are claimed to harbor pathogenic properties in cancer, particularly concerning changes in protein expression and splicing [31].

The significantly lower level of variants in FFPE samples than in fresh tissue (FT) in our study can be explained by fragmentation, which is often extensive in formalin fixed samples. Thus, FFPE tissues have a significantly lower amount of amplifiable DNA templates and need special preparation kits for library preparation [32].

Regarding mutational signature, all single base substitution signatures (S1, S5, S6, S12, S17, S23) were previously observed in liver cancer, but with variable

		LT6	LT8	LT10	LT11	LT13	LT14	LT16	LT17	LT18	LT19	LT20
Oncogenes	ALK	c.4196T>C					0.03					
	FLT3	c.1669G>A							0.026			
	FOXL2	c.536C>G			0.003							
	KIT	c.2863G>T										0.03
	MYCN	c.134_135del			Fs T3							
	PDGFRA	c.1432T>C			0.052							
	SETBP1	c.691G>C							0.061			
	SMO	c.518G>A							0.024			
Tumor Suppressor Genes	APC	c.5465T>A						0.378 T4				
	ATM	c.3161C>G						0.093				
	BRCA1	c.3024G>A										0.095
		c.4956G>A					0.111					
	CDH1	c.1896_1897delinsT				Fs T3						
							0.37 T1					
	CDKN2A	c.95T>A										
	CREBBP	c.6150_6151del				Fs T3						
	GATA3	c.480C>G		0.03								
	KMT2C	c.10979C>T							0.025			
	KMT2D	c.1074C>G					0.107					
		c.2293G>C	0.084									
	MEN1	c.512G>A							0.029			
	MSH2	c.56del				Fs T2						
	MSH6	c.4001+12_4001+15del										Fs T4
	PAX5	c.76del				Fs T3						
	PTCH1	c.163G>C							0.051			
	RUNX1	c.1009C>T		0.031								
	TET2	c.5347A>G								0.012		
		c.5396A>G									0.011	
	c.715G>A				0.012							
TNFAIP3	c.2090G>A					0.058					0.716 T1	
TP53	c.422G>A											

Fig. 5 Unique pathogenic variants in Oncogenes, tumor suppressor genes (TSGs) HCC with Phred score > 20, Fs = frameshift-truncation, Sc = Splice site, T1 = Tier1, T2 = Tier 2, T3 = Tier 3, T4 = Tier4. A higher CHASM + LIHC score (liver hepatocellular carcinoma) in colored areas indicates a higher possibility of being a driver mutation in HCC

frequencies [21]. Signatures SBS1 and SBS5 are clock-like mutational processes that increase with age progress. Signatures 12, 17, and 23 are of unknown reason. Signature SBS1 (associated with spontaneous deamination) and signature SBS5 (associated with the activity of transcription-coupled nucleotide excision repair) [33]. These mutational processes are active in both normal genomes as well as in tumor cells. Signature 6 is associated with defective DNA mismatch repair and

is found in microsatellite unstable tumors. It typically constitutes not more than 3% in cancers [34], but in our patients it constituted a high percentage with a median 14.2%. The mutational signature of FFPE samples is different from that of fresh samples. In their 2019 study, Bhagwate et al. also found that the DNA quality and quantity of FFPE samples are often sub-optimal, and resulting NGS-based genetics variant detections are prone to false positives, which could be the cause of the variation in mutational signature [35].

Table 5 Unique pathogenic variants with (CScape score > 0.5) unique pathogenic variants in SMGs TCGA HCC and Non-HCC

Chrom	Pos	Variant_note	Phred	Gene	Sequence_ontology	cDNA_change	Protein_change	Samples	CScape score
chr17	7,578,508	Tier1	101.81	TP53	missense	c.422G>A	p.Cys141Tyr	LT19_HCC	0.9312
chr5	1,293,625	Tier3	8.8584	TERT	stop_gained	c.1376G>A	p.Trp459Ter	LT08_HCC	0.9082
chr8	103,855,852	Tier3	30.607	AZIN1	missense	c.29A>G	p.Tyr10Cys	LT14_HCC	0.8998
chr19	10,600,008	Tier3	10.393	KEAP1	missense	c.1568G>A	p.Gly523Glu	LT07_HCC	0.8945
chr3	52,437,608	Tier3	6.2349	BAP1	missense	c.1553G>A	p.Arg518Gln	LT07_HCC	0.8922
chr3	178,952,085	Tier1	6.2381	PIK3CA	missense	c.3140A>G	p.His1047Arg	LT10_HCC	0.8043
chr8	103,845,284	Tier3	6.7846	AZIN1	missense	c.904G>A	p.Val302Ile	LT11_HCC	0.7754
chr2	21,227,996	Tier3	205.82	APOB	missense	c.11744C>T	p.Ser3915Phe	LT19_HCC	0.7374
chr1	27,100,124	Tier3	6.2383	ARID1A	missense	c.3920C>T	p.Pro1307Leu	LT07_HCC	0.6783
chr9	21,974,732	Tier2	25.112	CDKN2A	missense	c.95T>A	p.Leu32Gln	LT14_HCC	0.5713
chr1	27,094,369	Tier3	4.1526	ARID1A	missense	c.3077G>A	p.Arg1026His	LT07_Non	0.9154
chr16	354,405	Tier3	11.843	AXIN1	missense	c.1153C>T	p.Pro385Ser	LT07_Non	0.879
chr3	52,442,605	Tier2	5.7804	BAP1	frameshift	c.140_141insG	p.Ile47MetfsTer22	LT19_Non	0.856
chr3	52,442,545	Tier2	5.785	BAP1	frameshift	c.201dup	p.Asp68Ter	LT19_Non	0.85
chr2	178,098,885	Tier3	7.2747	NFE2L2	frameshift	c.160_161insA	p.Leu54HisfsTer2	LT10_Non	0.7653
chr16	348,239	Tier3	5.0519	AXIN1	frameshift	c.1267_1268insC	p.Glu423AlafsTer46	LT10_Non	0.6795
chr19	4,154,960	Tier3	5.8058	CREB3L3	missense	c.92A>G	p.Asp31Gly	LT10_Non	0.6625
chr2	21,239,431	Tier3	8.8517	APOB	missense	c.3212T>C	p.Val1071Ala	LT18_Non	0.6298
chr2	21,229,673	Tier3	7.8123	APOB	missense	c.10067T>C	p.Leu3356Pro	LT10_Non	0.588
chr8	10,465,934	Tier3	16.263	RP1L1	missense	c.5674A>G	p.Thr1892Ala	LT18_Non	0.5742

Hepatocellular carcinoma has a higher tumor mutation burden (TMB) than the average for other solid tumors. Tumor mutation burden is defined as the abundance of somatic mutations in a tumor, in the case of high TMB, immunotherapy can significantly improve overall survival than tumors with low TMB. The higher TMB differentiates the tumor from normal tissue, and exposes it to immune cells, thus it becomes more responsive to immunotherapy [36]. This is the reason we performed analysis of variants for both HCC and Non-HCC liver tissue to clarify the prevalence and type of variants present in both cancerous and non-cancerous liver tissue that increment TMB. Analysis of highly mutated genes in both HCC and Non-HCC revealed the presence of 8 highly mutated genes in HCC (*AHNAK2*, *MUC16*, *TTN*, *MUC6*, *MUC12*, *ZNF717*, *OBSCN*, *PDE4DIP*).

Mutations in *AHNAK2* are listed in pathological specimens and databases from The Cancer Genome Atlas (TCGA) [29]. *AHNAK2* (AHNAK nucleoprotein 2), also known as C14orf78, is a member of the AHNAK family. AHNAK mediates a negative regulation of cell growth and acts as tumor suppressor through potentiation of TGF β signaling. Upregulated *AHNAK2* activates the PI3K/AKT signaling pathway and promotes proliferation, migration, and invasion [37].

Analysis of highly mutated genes revealed that *MUC16* is highly rich in somatic variants in HCC liver tissue and is ranked third among HCC and Non-HCC regarding the

number of pathogenic variants arising in the gene in our study (supplement Tables 3 and 4). *MUC16*, an oncogene that encodes cancer antigen 125 (CA-125), sustains normal cell function, and its role in the development of numerous cancers is explained by being employed in activation of the p53 and DNA repair pathway. The critical role of the *MUC16* gene in HCC is highlighted as *MUC16* gene mutations which are enriched in various cancer-related pathways, such as cell cycle and metabolic processes. In addition, *MUC16* mutation significantly increases TMB and represents an independent marker with high predictive value for HCC [38, 39]. In our study, *AHNAK2*, *ZNF717*, *MAP2K3*, *HYDIN*, *OBSCN*, *PDE4DIP* are among the highly mutated genes. *TTN* and *OBSCN* were most abundant in HCC and Non-HCC respectively. Our results partially agree with Shen et al. (2020) who performed WES on liver tissues collected from 10 HCC Chinese patients. Among the 25 mutant genes in their study including a different gene profile, the highest mutation frequency was found in *HYDIN*, *TTN*, *OBSCN*, and *AHNAK2* [40].

In our data analysis, *TTN* and *OBSCN* were most frequent in HCC. In HCC samples, 11/13 (85%) samples had a commutant *OBSCN* and *TTN* while in Non-HCC 8/12 (67%) had mutation in both genes, with the remaining percentage showing only *OBSCN* pathogenic variants. Same observation was found previously in colorectal cancer (CRC) patients in TCGA

Table 6 Heatmap showing TCGA SMGs unique pathogenic variants among HCC and Non-HCC patients samples and their frequency

Genes	LT6	LT7	LT7n	LT8	LT8n	LT10	LT10n	LT11	LT11n	LT13	LT13n	LT14	LT14n	LT16	LT17	LT17n	LT18	LT18n	LT19	LT19n	LT20	LT20n	Freq HCC	Freq Non	
RP1L1	1	2	1			1	9	1	5	2	4	2		2	2	1					1	1	3	69.20%	50%
APOB						1	6	1	2	1		3	1	4					4	1	1	1		53.80%	41.70%
AXIN1	2	1	3			1	1	1	2	1				1		1								46.20%	33.30%
TERT		1	1	1	1			1	1				1	2		1				1	1			46.20%	41.70%
AHCTF1						4	3			2		2		1				1			3			38.40%	16.70%
KEAP1		1				3	1			1		1												30.80%	8.30%
NFE2L2							2	2		2									1		1	1		30.80%	16.70%
PIK3CA						1	2	1				1							1					30.80%	8.30%
ARID1A	1	2	1				4		4	3											2			23.10%	33.30%
CREB3L3		2	1				1					1	1		1	1								23.10%	33.30%
GPATCH4								1		1		1												23.10%	–
IL6ST									1			2			1					1				23.10%	16.70%
LZTR1						1	1			1		2	1								1			23.10%	16.70%
RB1								1				1							1		1			23.10%	8.30%
ARID2						1	1					3												15.40%	8.30%
AZIN1								1				1												15.40%	–
BAP1		1				1		2				1	1							3				15.40%	8.30%
CTNNB1							1					1							1					15.40%	8.30%
EEF1A1								1		1														15.40%	–
ACVR2A												1												7.60%	–
CDKN2A												2												7.60%	–
KRAS												1	1											7.60%	8.30%
TP53									1										1			1		7.60%	16.70%
ALB									1															–	8.30%
Grand Total	4	10	7	1	1	14	32	13	17	15	4	26	6	10	4	4	2	1	8	8	7	9			

		LT10N	LT11N	LT13N	LT14N	LT16N	LT17N	LT18N	LT19N	LT20N
Oncogenes	BCL2	c.119_120del	Fs T3							
	DNMT1	c.1782_1783delinsG	Fs T3							
	DNMT3A	c.1798G>T		0.159						
	EGFR	c.2962C>A							0.077	
	FGFR2	c.68C>A							0.08	
	FGFR3	c.1156T>C	0.107							
		c.158G>C								0.065
	FOXL2	c.536del	Fs T3							
	MYC	c.553G>A				0.013				
	NRAS	c.510del						Fs T3		
Tumor Suppressor Genes	ATM	c.2290A>G						0.065		0.047
		c.4424A>G						0.06		
		c.53A>G						0.049		
		c.6348-2A>G								Ss T1
		c.670A>G								0.047
	BRCA1	c.2099T>C								0.107
		c.3056T>C						0.114		
		c.3113A>G	0.103							
	BRCA2	c.5744C>T								0.09
	CASP8	c.853G>C								0.055
	CDH1	c.271T>C								0.124
	EP300	c.5887G>T	0.184							
	HNF1A	c.293C>T							0.324 T4	
		c.864del					Fs T3			
		c.872del					Fs T3			
	KMT2D	c.5135del						Fs T2		
		c.5135_5136del		Fs T2						
		c.8713_8715delinsG		Fs T2						
	NF1	c.5216T>C				0.275 T3				
	PRDM1	c.1061G>A		0.043						
	c.220G>A	0.039								

Fig. 6 Unique pathogenic variants in Oncogenes, tumor suppressor genes (TSGs) Non- HCC with Phred score > 20, Fs = frameshift-truncation, Ss = Splice site, T1 = Tier1, T2 = Tier 2, T3 = Tier 3, T4 = Tier4. A higher CHASM + LIHC score (liver hepatocellular carcinoma) in colored areas (CHASMplus LIHC score) indicates a higher possibility of being a driver mutation in Non-HCC

study, *TTN* and *OBSCN* were commonly mutated, and mutations correlated with higher TMB and favorable overall survival. Patients with the commutation of *TTN* and *OBSCN* were categorized as ‘Double-Hit’, patients with only one gene mutation *TTN* or *OBSCN* were labelled ‘Single-Hit’, and patients with both genes

wild-type were categorized ‘Double-WT’. Double-Hit group revealed low tendency to malignant events, and highest TMB, immune cells infiltration abundance, as well as immune checkpoints expression compared with the other two phenotypes. This finding may extend to HCC but needs exploration through further studies;

Table 7 Enriched Kegg pathways in combined HCC samples

Term	Gene count	%	P-values	Individual samples $p < 0.05$	Individual samples $p < 0.1$	Freq %
ECM-receptor interaction	50	0.8	1.2E-6	LT6, LT7, LT10, LT13, LT14, LT16, LT19, LT20		61%
Focal adhesion	86	1.4	3.6E-4	LT6, LT11, LT13, LT14, LT16, LT17		46%
Notch signaling	33	0.5	4.1E-4	LT7, LT8,	LT16	23%
Calcium signaling	96	1.6	9.3E-3	LT7, LT8	LT17	23%
Wnt signaling	68	1.1	1.4E-2	LT8	LT11	15%
PI3K-Akt signaling	130	2.2	1.5E-2	LT13, LT14	LT10, LT19, LT20	38.4%
Apelin signaling	39	1.0	2.3E-2	LT8, LT13		15%
Hippo signaling	12	1.7	1.5E-2	LT7		7.5%
Hedgehog signaling	11	0.7	2.0E-2	LT13		7.5%
MAPK signaling	20	2.2	3.2E-2	LT14		7.5%

researchers suggest ‘immune-hot’ category of tumors to have better immunotherapeutic efficacy and as a result a more favorable prognosis [41].

The HCC mutational landscape is characterized by both pronounced intra and inter-tumoral heterogeneity with a lack of a representative actionable oncogenic driver. Gene-specific filtering was performed on our WES data in both HCC and Non-HCC for the 26 significantly mutated genes in TCGA study [42] to expand data interrogation across the entire exome, and to perform candidate gene analysis based on what we obtained from up-to-date curated databases [43]. Although the Phred score for some of these variants was low, in most variants due to homopolymers errors by ion Proton semiconductor-based sequencing detection method, they passed variant assessment and had an accepted depth of coverage [44]. HCC development is mainly driven by inactivating mutations in various tumor-suppressor genes as *TP53*, *AXIN1*, *ARID1A*, *ARID2*, and *CDKN2A*; mutations in oncogenes as *CTNNB1*, *PIK3CA*, *KRAS*, *NRAS*, *NEF2L2*, which predispose hepatocytes to accumulate additional oncogenic changes that drive cancer initiation and tumorigenesis [42]. Our study shows concordant results with genes *TP53*, *TERT*, *Azin1*, *KEAP1*, *BAP1*, *PIK3CA*, *APOB*, *ARID1A*, *CDKN2A*, *AXIN1*, *NFE2L2*, *CREB3L3*, and *RPIL1* showing variants with a high probability of being driver mutations in a variable number of our HCC cases having CScape score > 0.5 [30].

Exploring The Cancer Genome Atlas Significantly Mutated Genes (TCGA SMGs), in our study the most frequently mutated genes in HCC samples were *APOB* (53%), *RPIL1* (69%), *AHCTF1* (46%), *AXIN1* (46%) and *AHCTF1* (38%), *KEAP1* (31%), *NEF2L2* (31%), and *PIK3CA* (31%). The most frequently mutated genes in Non-HCC samples in our study were *RPIL1* (50%), *APOB* (41.7%), *TERT* (41.7%), *ARID1A* (33%), *CREB3L3* (33%), and *AXIN1* (33%), some of the most established

drivers of HCC [42]. In accordance with our results, mutated genes in our study were among the most frequently mutated group of HCC driver genes in TCGA. However, in TCGA the two most frequently mutated genes ($> 25\%$ of total cases), in their study on 363 HCC cases were tumor suppressor gene *TP53* and the WNT pathway oncogene *CTNNB1* [30]. Genes *TP53* had unique pathogenic coding variants in 7.6% of HCC samples and 16.7% of Non-HCC, while *CTNNB1* in 15.4% of HCC and 8.3% of Non-HCC. Genes involved in Wnt pathway as *AXIN1* showed unique pathogenic variants in 46% of our HCC samples and were mutually exclusive to the activating β -catenin mutations except in one Non-HCC sample which showed both *AXIN1* and *CTNNB1* mutations [45]. The *AXIN1* gene, on the other hand, is a negative regulator of the Wnt/ β -catenin pathway. Mutually exclusive mutations occurring in AXINS are driver mutations that drive hepatocarcinogenesis in the stage of low-grade dysplastic nodules in cirrhotic liver. In their study, TCGA reported a low percentage of both *NEF2L2* (3%) and *KEAP1* (5%) and highlighted their vital role in cellular antioxidant defenses [9].

Variants were observed in HCC samples in TCGA SMGs in *ARID1A* (23%), *CREB3L3* (23%), *GPATCH4* (23%), *IL6ST* (23%), *LZTR1* (23%), *RB1* (23%), *ARID2* (15%), *AZINI* (15.4%), *BAP1* (15.4%), *CTNNB1* (15.4%), *EEF1A1* (15.4%), *CDKN2A* (7.6%), *ACVR2A* (7.6%), *KRAS* (7.6%), and *TP53* (7.6%). In agreement with our results, driver mutational events were observed in TCGA study at the level of *LZTR1*, *EEF1A1*, *ARID2*, *AZINI*, *GPATCH4*, *CREB3L3*, and *ACVR2A* genes [29]. Shibata, in 2021, added that low frequency mutated driver genes may trigger specific oncogenic phenotypes such as aggressive growth, invasiveness, or metastasis [46]. Driver mutations in *ARID1A* and *ARID2* which are involved in chromatin remodeling occur early in the stage of high-grade dysplastic nodules preceding the

Table 8 Tier1 and Tier2 variants in HCC and Non-HCC samples (GRCH37) all heterozygous, population frequency < 0.1

	Variant	Phred	Position	Sequence ontology/ VAF	ACMG category	HCC LT/Non-HCC LTN (VAF)
1	<i>TP53</i> c.422G>A NM_000546.6	101	chr17 7,578,508	Missense	Tier1	LT19 (22.95%)
2	<i>CDKN2A</i> c.95 T> A NM_000077.5	25	chr9 21,974,732	Missense	Tier1	LT14 (7.14%)
3	<i>MSH2</i> c.56del NM_000251.3	37.6	chr2 47,630,385	Frameshift	Tier2	LT13(18.18%)
4	<i>KMT2D</i> c.8713_8715delinsG NM_003482.4	20.4	chr12 49,432,424	Frameshift	Tier2 HP	LT11N (4.76%)
5	<i>KMT2D</i> c.5135_5136del NM_003482.4	17.3	chr12 4,943,803	Frameshift	Tier2 HP	LT11N (3.86%)
6	<i>KMT2D</i> c.5135del NM_003482.4	27.6	chr12 49,438,036	Frameshift	Tier2 HP	LT17N (10.29%)
7	<i>ATM</i> c.6348-2A>G NM_000051.4	23	chr11 108,190,679	Splice site	Tier1	LT20N (4.11%)
8	<i>KIT</i> c.1621A>C p.Met541Leu NM_000222.3	119	chr4: 55,593,464	Missense	Tier2	LT11, 18,19 (22%, 43%, 52%)
9	<i>KMT2D</i> c.8455C>T NM_003482.4	8.7	Chr12 49,432,684	Stop_gained	Tier2	LT7 (3.33%)
10	<i>KMT2D</i> c.3553C>T NM_003482.4	11.8	Chr12 49,443,818	Stop_gained	Tier2	LT7 (4.29%)
11	<i>NOTCH1</i> c.1773C>A NM_017617.5	8.9	Chr9 139,410,065	Stop_gained	Tier1	LT8N (3.23%)
12	<i>KMT2C</i> c.1084_1085insC NM_170606.3	8.3	chr7-151,962,222	Frameshift	Tier2	LT10 (3.28%)
13	<i>PIK3CA</i> c.1325_1326insG NM_006218.4	8.9	Chr3 178,928,048	Frameshift	Tier1	LT11 (3.57%)
14	<i>KMT2D</i> c.9279_9280insG NM_003482.4	7.7	Chr12 49,431,859	Frameshift	Tier2	LT11N (2.2%)
15	<i>KIT</i> c.1149dup NM_000222.3	8.5	Chr4 55,575,619	Frameshift	Tier1	LT11N (4.76%)
16	<i>SMARCA4</i> c.3392del NM_003072.5	17.7	Chr 19 11,141,415	Frameshift	Tier2	LT13 (7.73%)
17	<i>KMT2D</i> c.15838_15839insC NM_003482.4	7.7	Chr12 49,418,675	Frameshift	Tier2	LT14 (1.75%)
18	<i>SMARCA4</i> c.1834_1835insG NM_003072.5	7	Chr19 11,113,727	Frameshift	Tier2	LT14 (1.85%)
19	<i>NOTCH1</i> c.3763_3764insC NM_017617.5	7.4	Chr9 139,401,305	Frameshift	Tier1	LT17 (2.82%)
20	<i>ATM</i> c.5870_5871insC NM_000051.4	8	Chr11 108,180,994	Frameshift	Tier1	LT18N (3.17%)
21	<i>PTEN</i> c.812T>C NM_000314.8	7.3	chr10 89,720,661	Missense	Tier2	LT18N (2.78%)
22	<i>MSH2</i> c.577C> T NM_000251.3	7.3	Chr2 47,637,443	Stop_gained	Tier2	LT19 (2.78%)
23	<i>PTCH1</i> c.1963C>T NM_000264.5	8.5	Chr9 98,231,320	Stop-gained	Tier1	LT7N (3.23%)

development of HCC. One of the key pathways in HCC included cell cycle regulatory pathways driven by mutations in *RBI*, *CDKN2A* [9]. We found no variants in *ALB*, Shibata mentioned the uncertain role of frequent mutations of *ALB* and *APOB* in HCC. He explained that both mutations were enriched in indels and both genes are highly expressed in hepatocytes, these indels could be caused by replication errors [47]. In agreement with his explanation, out of 15 variants in *APOB* in our study, 11 were indels in HCC and 8/14 variants in Non-HCC samples were frameshift caused by indels. Both *ALB* and *APOB* genes are key mediators of hepatocyte function in the secretion of albumin and VLDL. Their role requires a high portion of hepatocyte transcriptional, translational, and energy supplies. This might explain *APOB* mutation and suppression by the malignant hepatocyte to reserve resources for cell division requirements [46].

Analysis of variants regarding the Cancer Genome Landscape revealed the presence of Tier1 variants in TP53 and CDKN2A, both are driver genes in HCC [41], in addition to Tier 2 variant in MSH2, the DNA mismatch repair gene whose defects can contribute to cancer development. In their 2018 study, Zhu et al., highlighted the role of rs2303428 of MSH2 in HCC prognosis [48]. This is an intron variant that was observed in our study in both HCC (VAF 63%) and non-HCC (VAF 54%) samples of one patient HCV-HCC. It is mainly identified in constitutional germline dependent hereditary cancers and as a somatic mutation in some sporadic cancers. As we traced in our study exome, we filtered for pathogenic coding variants in addition to splice site variants. Further studies are needed to determine the impact on prognosis. In addition, a splice site variant Tier 1 was identified in *ATM* gene, and 2 Tier 2 variants frameshift in *KMT2D* in Non-HCC samples. These tumor suppressor genes represent driver mutations in HCC, previous studies revealed many low-frequency somatic mutations that affect multiple genes, including cell cycle control as *ATM* in 6% of HCC patients, and recurrent inactivating mutations of members of the chromatin remodeling gene family as *KMT2D* in 6% of HCC patients [27].

Data analysis of the identified KEGG pathways for somatic unique variants in HCC samples highlights mutated genes' roles during tumorigenesis, revealing biological processes and pathways implicated in carcinogenesis.

Extracellular matrix ECM-receptor interaction (61%) and Focal adhesions (46%) are significantly enriched in our HCC samples. Focal adhesions are structural links between the extracellular matrix (ECM) and actin cytoskeleton. Integrins interact with multiple proteins at cell-ECM adhesion sites forming focal adhesions (FAs). These adhesions orchestrate significant cancer related

functions including cell proliferation and survival, cell invasion and epithelial mesenchymal transition. Understanding the pathogenesis of tumor cell motility can pave the way to effective therapeutic targeting to prevent cancer progression [49]. Calcium signaling was enriched in 23% of HCC samples, this pathway is reported to be associated with liver-specific diseases such as HCC, cholestasis, hepatitis, and nonalcoholic fatty liver disease (NAFLD). Calcium signaling is coordinated by ~1600 genes, the ultimate role of these genes is to maintain the intracellular calcium homeostasis and normal cell function. Altered calcium signaling genes expression is implicated in cancer hallmarks, such as altered cell metabolism, sustained cell proliferation, cell death resistance, angiogenesis, invasion, and metastasis [50].

Pathways PIK3AKT and Wnt had the highest number of genes enriched (130 and 68, respectively) with PIK3AKT having a frequency 38.4% in HCC samples. Regarding PI3K-Akt, several studies documented mutations of the phosphatidylinositol 3-kinase (PI3K)/the serine-threonine protein kinase (Akt)/mammalian target of the rapamycin (mTOR) signaling pathway in HCC. The PI3K/Akt/mTOR pathway is an important signaling mechanism that regulates the cell cycle, proliferation, apoptosis, and metabolism. The pathway is often dysregulated in HCC which promotes the survival and proliferation of tumor cells [51].

Signaling pathway Notch is enriched in 23% of HCC patients. Mutation in target genes of the Notch pathway is reported in HCC and it is notable that the Notch pathway has controversial effects on HCC. This pathway cross-talks with the Wnt pathway for cancer stem cell (CSC) maintenance, the PI3K/mTOR pathways for HCC proliferation, and the VEGF pathway for angiogenesis [52].

Apelin and Wnt signaling pathways are enriched in 15% of HCC patients. Activated β -catenin activates the transcription of target genes modulating the process of carcinogenesis. These genes are involved in CSC maintenance, proliferation, and epithelial mesenchymal transition (EMT) [53]. The apelin signaling pathway is a G protein-coupled receptor (GPCR) pathway that plays a crucial role in regulating various physiological processes such as angiogenesis, and energy metabolism that are involved in carcinogenesis. The apelin signaling pathway interacts with other pathways as the Wnt/ β -catenin pathway, the PI3K/Akt/mTOR pathway, and the Hippo pathway to regulate the development of HCC [54].

Signaling pathways Hippo, Hedgehog (Hh) and MAPK were revealed to be enriched in 3 HCC patients. Hippo is a classical kinase cascade that phosphorylates the Mst1/2-sav1 complex and activates the phosphorylation of the Lats1/2-mob1A/B complex for inactivating Yap and Taz. Yap/Taz is the main effector molecule, which

is downstream of the Hippo pathway, and its abnormal activation is related to a variety of human cancers including HCC [55]. In adult healthy liver, Hh signaling is inactive, because mature hepatocytes hardly express Hh ligands. Hh signaling is reactivated in liver diseases, activation enhances transition of quiescent hepatic stellate cells (HSCs) to myofibroblast (MF), which regenerate the liver epithelial cells. The Hh pathway can be activated by inactivating mutations of *PTCH1* [56]. The mitogen-activated protein kinase/extracellular signal-regulated kinase (MAPK-ERK) is one of the molecular signaling pathways that are critical to tumor initiation, progression, and metastasis in HCC. It is a cascade of protein kinases that transmits signals from the cell surface to the nucleus. In HCC, the MAPK/ERK signaling pathway is activated in more than 50% of human HCC cases [57].

In our study, we demonstrated the presence of different unique mutations in every patient between HCC and Non-HCC samples, and interpatient molecular differences between different studied patients. Tumor heterogeneity is a hallmark of hepatocellular carcinomas (HCCs), that poses a significant challenge to the development of effective therapeutic solutions in HCC. Inter-tumor heterogeneity that can be related to de novo independent carcinogenesis on a background of cirrhosis and/or intrahepatic metastasis. The presence of variants in Non-HCC can be attributed to either intrahepatic metastases which is reported in previous studies in 20 to 40% of patients, or de novo carcinogenesis on cirrhosis [9]. We explored gene variants in significant pathways, and we demonstrated the presence of considerable heterogeneity in different liver tissues HCC and Non-HCC in the same patient at the DNA sequence level. These patients belong to the same Geographic region but have different etiologies, however they shared most KEGG pathways, except for Hh pathway in HBV HCC. Somatic mutations in similar loci of genes that are clinically actionable even though of different sequence ontology may serve as important therapeutic targets [58].

Tier 1 and Tier 2 mutations

All variants in genes showing clinically actionable Tier 1 and Tier 2 variants that represent driver mutations in HCC are involved in driver pathways for HCC which we discussed earlier PI3K/mTOR, Wnt, NOTCH, Hedgehog, and MAPK [52]. In addition, some are determined through cell cycle control, chromatin remodeling and oxidative stress to be involved in the process of carcinogenesis in HCC [28]. We extended the list in supplement files, to include variants within driver genes that are abundant on COSMIC and are targetable [24, 52]. Although frameshift variants represented only 1.6% of all variants in WES, they all lied within driver genes

and genes implicated in the process of carcinogenesis [28] in our patients and represented the dominant sequence ontology among pathogenic variants. Some of them on region viewer or on Franklin were found to lie in homopolymers regions [43]. These variants in addition to a considerable number of medium VAF, high and medium confidence Tier 3 variants in every HCC patient require further assessment and consideration of their clinical significance.

Conclusion

Mutational signature was mostly found in S1, S5, S6, and S12 in HCC. Analysis of highly mutated genes revealed the presence of 10 common highly mutated genes in HCC and Non-HCC (*AHNAK2*, *MUC6*, *MUC16*, *TTN*, *ZNF17*, *FLG*, *MUC12*, *OBSCN*, *PDE4DIP*, *MUC5b*, and *HYDIN*). Among the 26 significantly mutated HCC genes identified by TCGA, *APOB* and *RPIL1* showed the highest number of mutations in both HCC and Non-HCC tissues. Tier 1, Tier 2 variants in TCGA SMGs in HCC and Non-HCC (*TP53*, *PIK3CA*, *CDKN2A*, and *BAP1*). Cancer Genome Landscape analysis revealed multiple variants added (*MSH2*) in HCC and (*KMT2D* and *ATM*) in Non-HCC. For KEGG analysis, among the significantly annotated clusters in HCC were Notch signaling, Wnt signaling, PI3K-AKT pathway, Hippo signaling, Apelin signaling, Hedgehog (Hh) signaling, and MAPK signaling, in addition to ECM-receptor interaction, focal adhesion, and calcium signaling. Tier 1 and Tier 2 variants *KIT*, *KMT2D*, *NOTCH1*, *KMT2C*, *PIK3CA*, *KIT*, *SMARCA4*, *ATM*, *PTEN*, *MSH2*, and *PTCH1* low frequency variants in both HCC and Non-HCC. Further assessment and confirmation for these variants and other Tier 3 ones are recommended.

Abbreviations

HCC	Hepatocellular carcinoma
HCV	Hepatitis C virus
ITH	Intra-tumor heterogeneity
NGS	Next-generation sequencing
WES	Whole exome sequencing
SNPs	Single nucleotide polymorphisms
EASL	European association for study of liver diseases
UCSF	University of California San Francisco criteria
BCLC	Barcelona clinic for cancer staging
CR	Complete response
ST	Stable disease
mRECIST	Modified Response Evaluation Criteria in Solid Tumors (RECIST) criteria
FFPE	Fresh frozen paraffin embedded
TCGA	The Cancer Genome Atlas

Supplementary Information

The online version contains supplementary material available at <https://doi.org/10.1186/s12920-024-01965-w>.

Supplementary Material 1.

Acknowledgements

All Staff members of Ain Shams Center for Organ Transplantation (ASCOT).

Authors' contributions

P.H.K and M.E.M chose the idea, R.M., D.A., R.A., K.M. did the lab workup, P.H.K. M.F., M.A. prepared the figures, P.H.K., R.M., D.A. prepared the tables, P.H.K., I.M. wrote the main manuscript, I.M., M.S., Y.M. revised the clinical data and follow up of patients, M.E.M., M.B. did the surgical procedures, M.I. prepared the pathological specimens and read the pathology, A.A. analyzed the data files for somatic extraction, M.A.H. supervised the bioinformatics and raw data files and supervised the work, P.H.K. do the data analysis., performed data analysis to assign the driver mutations and mutational signatures and pathways S.E.K supervised and consultant the project. All authors reviewed the manuscript.

Funding

This work was supported by Science and Technology Development Fund (STDF), Basic and Applied Research Grant Call 7 (BARG Call 7, Project ID:38229).

Availability of data and material

The data can be available on reasonable request from the corresponding author.

Declarations

Ethics approval and consent to participate

This study was reviewed and approved by the Research Ethics Committee of the Faculty of Medicine, Ain Shams University (FMASU R92/2020). All participants have assigned written informed consent form to participate in this study. The study was performed in accordance with the 1964 Declaration of Helsinki and all subsequent revisions.

Consent for publication

Not applicable.

Competing interests

The authors declare no competing interests.

Author details

¹Clinical Pathology Department, Faculty of Medicine, Ain Shams University, Cairo, Egypt. ²Tropical Medicine Department, Faculty of Medicine, Ain Shams University, Cairo, Egypt. ³Hepato-Pancreatico-Biliary Surgery Department and liver Transplantation, Faculty of Medicine, Ain Shams University, Cairo, Egypt. ⁴Pathology Department, Faculty of Medicine, Ain Shams University, Cairo, Egypt. ⁵Institute of Cancer and Genomic Sciences, College of Medical and Dental Sciences, University of Birmingham Dubai Campus, Dubai, United Arab Emirates. ⁶Bioinformatics Group, Center for Informatics Science(CIS), School of Information Technology and Computer Science(ITCS), Nile University, Giza, Egypt. ⁷School of Biosciences, University of Sheffield, Sheffield, UK.

Received: 2 February 2024 Accepted: 17 July 2024

Published online: 09 August 2024

References

- Sung H, Ferlay J, Siegel RL, et al. Global cancer statistics: GLOBOCAN estimates of incidence and mortality worldwide for 36 cancers in 185 countries. *CA Cancer J Clin*. 2021;71:209–49.
- Elghazaly H, GabAllah A, Eldin NB. P-019 Clinic-pathological pattern of hepatocellular carcinoma (HCC) in Egypt. *Ann Oncol*. 2018;29. <https://doi.org/10.1093/annonc/mdy151.018>.
- Wang H, Zhou H, Li X, Wang P, Liu G, Liu W, et al. Detection of tumor-related biomarkers in hepatocellular carcinoma patients by sequencing circulating cell-free DNA. *Clin Oncol*. 2019;4:1645.
- Maloberti T, De Leo A, Sanza V, Gruppioni E, Altimari A, Riefolo M, Visani M, Malvi D, D'Errico A, Tallini G, Vasuri F, de Biase D. Correlation of molecular alterations with pathological features in hepatocellular carcinoma: literature review and experience of an Italian center. *World J Gastroenterol*. 2022;28(25):2854–66.
- European Association for the Study of the Liver. EASL recommendations on treatment of hepatitis C. *J Hepatol*. 2018;69(2):461–511.
- Markou A, Tzanikou E, Lianidou E. The potential of liquid biopsy in the management of cancer patients. *Semin Cancer Biol*. 2022;84:69–79. <https://doi.org/10.1016/j.semcancer.2022.03.013>
- Ganesamoorthy D, Robertson AJ, Chen W, Hall MB, Cao MD, Ferguson K, Coin LJ. Whole genome deep sequencing analysis of cell-free DNA in samples with low tumour content. *BMC Cancer*. 2022;22(1):1–13.
- Kunadirek P, Chuaypen N, Jenjaroenpun P, Wongsurawat T, Pinjaroen N, Sirichindakul P, Tangkijvanich P. Cell-free DNA analysis by whole-exome sequencing for hepatocellular carcinoma: a pilot study in Thailand. *Cancers*. 2021;13(9):2229.
- Rebouissou S, Nault JC. Advances in molecular classification and precision oncology in hepatocellular carcinoma. *J Hepatol*. 2020;72(2):215–29. <https://doi.org/10.1016/j.jhep.2019.08.017>.
- Imamura T, Okamura Y, Ohshima K, et al. Overview and clinical significance of multiple mutations in individual genes in hepatocellular carcinoma. *BMC Cancer*. 2022;22:1046. <https://doi.org/10.1186/s12885-022-10143-z>.
- Rabbani B, Tekin M, Mahdieh N. The promise of whole-exome sequencing in medical genetics. *J Hum Genet*. 2014;59(1):5–15.
- Botstein D, Risch N. (2003): Discovering genotypes underlying human phenotypes: past successes for mendelian disease, future approaches for complex disease. *Nat Genet*. 2003;33(Suppl):228–37.
- Tetreault M, Barek E, Nadaf J, Alirezaie N, Majewski J. Whole-exome sequencing as a diagnostic tool: current challenges and future opportunities. *Expert Rev Mol Diagn*. 2015;15(6):749–60.
- Mazzaferro V, et al. Liver transplantation for the treatment of small hepatocellular carcinomas in patients with cirrhosis. *New England J Med*. 1996;334(11). <https://doi.org/10.1056/nejm199603143341104>.
- Yao FY et al. Liver transplantation for hepatocellular carcinoma: expansion of the tumor size limits does not adversely impact survival. *Hepatology*. 2001;33(6). <https://doi.org/10.1053/jhep.2001.24563>.
- Llovet JM, Lencioni R. mRECIST for HCC: performance and novel refinements. *J Hepatol*. 2020;72(2):288–306. <https://doi.org/10.1016/j.jhep.2019.09.026>. PMID: 31954493.
- Reig M, Forner A, Rimola J, Ferrer-Fàbrega J, Burrel M, Garcia-Criado Á, Kelley RK, Galle PR, Mazzaferro V, Salem R, Sangro B, Singal AG, Vogel A, Fuster J, Ayuso C, Bruix J (2022): BCLC strategy for prognosis prediction and treatment recommendation: the 2022 update. *J Hepatol*. 2022;76(3):681–93. <https://doi.org/10.1016/j.jhep.2021.11.018>. Epub 2021 Nov 19 PMID: 34801630.
- Yau T, Tang VY, Yao TJ, Fan ST, Lo CM, Poon RT. Development of Hong Kong liver cancer staging system with treatment stratification for patients with hepatocellular carcinoma. *Gastroenterology*. 2014;146:1691–1700.e3 PMID: 24583061.
- Lucena-Aguilar G, Sánchez-López AM, Barberán-Aceituno C, Carrillo-Ávila JA, López-Guerrero JA, Aguilar-Quesada R. DNA source selection for downstream applications based on DNA quality indicators analysis. *Biopreserv Biobank*. 2016;14(4):264–70. <https://doi.org/10.1089/bio.2015.0064>. Epub 2016 May 9. PMID: 27158753; PMCID: PMC4991598.
- Cingolani P, Platts A, Wang LL, Coon M, Nguyen T, Wang L, Land SJ, Lu X, Ruden DM. A program for annotating and predicting the effects of single nucleotide polymorphisms, SnpEff. *Fly*. 2012;6(2):80â–92. <https://doi.org/10.4161/fly.19695>.
- Lee J, Lee AJ, Lee JK, Park J, Kwon Y, Park S, Chun H, Ju YS, Hong D. Mutalisk: a web-based somatic MUTation AnaLysis toolKit for genomic, transcriptional and epigenomic signatures. *Nucleic Acids Res*. 2018;46(w1):W102–8. <https://doi.org/10.1093/nar/gky406>.
- Pagel KA, et al. Integrated informatics analysis of cancer-related variants. *JCO Clinical Cancer Informatics*. 2020;4:310–7.
- Carter H, et al. Cancer-specific high-throughput annotation of somatic mutations: computational prediction of driver missense mutations. *Cancer Res*. 2009;69:6660–7.
- Van Allen EM, Wagle N, Stojanov P, et al. Whole-exome sequencing and clinical interpretation of formalin-fixed, paraffin-embedded tumor samples to guide precision cancer medicine. *Nat Med*. 2014;20(6):682.
- Vogelstein B, Papadopoulos N, Velculescu VE, Zhou S, Diaz LA, Kinzler KW. Cancer genome landscapes. *Science*. 2013;339(6127):1546–58.
- Li MM, Datto M, Duncavage EJ, Kulkarni S, Lindeman NI, Roy S, Tsimberidou AM, Vnencak-Jones CL, Wolff DJ, Younes A, Nikiforova MN. Standards

- and guidelines for the interpretation and reporting of sequence variants in cancer: a joint consensus recommendation of the association for molecular pathology, American Society of Clinical Oncology, and College of American Pathologists. *J Mol Diagn*. 2017;19(1):4–23. <https://doi.org/10.1016/j.jmoldx.2016.10.002>. PMID: 27993330; PMCID: PMC5707196.
27. Sherman BT, Hao M, Qiu J, Jiao X, Baseler MW, Lane HC, Imamichi T, Chang W. DAVID: a web server for functional enrichment analysis and functional annotation of gene lists (2021 update). *Nucleic Acids Res*. 2022;50(W1):W216–21. <https://doi.org/10.1093/nar/gkac194>.
 28. Schulze K, Nault JC, Villanueva A. Genetic profiling of hepatocellular carcinoma using next-generation sequencing. *J Hepatol*. 2016;65(5):1031–42. <https://doi.org/10.1016/j.jhep.2016.05.035>. Epub 2016 Jun 2 PMID: 27262756.
 29. Cancer Genome Atlas Research Network. Electronic address: wheeler@bcm.edu; Cancer Genome Atlas Research Network. Comprehensive and Integrative Genomic Characterization of Hepatocellular Carcinoma. *Cell*. 2017;169(7):1327–1341.e23. <https://doi.org/10.1016/j.cell.2017.05.046>. PMID: 28622513; PMCID: PMC5680778.
 30. Rogers MF, Shihab H, Gaunt TR, Campbell C. CScape: a tool for predicting oncogenic single-point mutations in the cancer genome. *Nature Scientific Rep*. 2017. <http://cscap.biocompute.org.uk/>
 31. Sauna ZE, Kimchi-Sarfaty C. Understanding the contribution of synonymous mutations to human disease. *Nat Rev Genet*. 2011;12(10):683–91.
 32. Do H, Dobrovic A. Sequence artifacts in DNA from formalin-fixed tissues: causes and strategies for minimization. *Clin Chem*. 2015;61(1):64–71. <https://doi.org/10.1373/clinchem.2014.223040>.
 33. Alexandrov LB, et al. Clock-like mutational processes in human somatic cells. *Nat Genet*. 2015;47:1402–7.
 34. Zhuravleva E, O'Rourke CJ, Andersen JB. Mutational signatures and processes in hepatobiliary cancers. *Nat Rev Gastroenterol Hepatol*. 2022;19:367–82. <https://doi.org/10.1038/s41575-022-00587-w>.
 35. Bhagwate AV, Liu Y, Winham SJ, et al. Bioinformatics and DNA-extraction strategies to reliably detect genetic variants from FFPE breast tissue samples. *BMC Genomics*. 2019;20:689. <https://doi.org/10.1186/s12864-019-6056-8>.
 36. Xie C, Wu H, Pan T, Zheng X, Yang X, Zhang G, Lian Y, Lin J, Peng L. A novel panel based on immune infiltration and tumor mutational burden for prognostic prediction in hepatocellular carcinoma. *Aging (Albany NY)*. 2021;10(13(6)):8563–8587. <https://doi.org/10.18632/aging.202670>. Epub 2021 Mar 10. PMID: 33714200; PMCID: PMC8034943.
 37. Wang DW, Zheng HZ, Cha N, Zhang XJ, Zheng M, Chen MM, Tian LX. Down-regulation of AHNK2 inhibits cell proliferation, migration and invasion through inactivating the MAPK pathway in lung adenocarcinoma. *Technol Cancer Res Treat*. 2020;19:1533033820957006. <https://doi.org/10.1177/1533033820957006>. PMID: 33000678; PMCID: PMC7533926.
 38. Liu B, Dong Z, Lu Y, Ma J, Ma Z, Wang H. Prognostic value of MUC16 mutation and its correlation with immunity in hepatocellular carcinoma patients. *Evid Based Complement Alternat Med*. 2022;3478861. <https://doi.org/10.1155/2022/3478861>. PMID: 36034941; PMCID: PMC9410786.
 39. Huang Y, Huang X, Zeng J, Lin J. Knockdown of MUC16 (CA125) enhances the migration and invasion of hepatocellular carcinoma cells. *Front Oncol*. 2021;11:667669. <https://doi.org/10.3389/fonc.2021.667669>. PMID: 34150633; PMCID: PMC8208084.
 40. Shen J, Qi L, Zou Z, Du J, Kong W, Zhao L, Wei J, Lin L, Ren M, Liu B. Identification of a novel gene signature for the prediction of recurrence in HCC patients by machine learning of genome-wide databases. *Sci Rep*. 2020;10(1):4435. <https://doi.org/10.1038/s41598-020-61298-3>. PMID: 32157118; PMCID: PMC7064516.
 41. Liu Z, Wang L, Guo C, Liu L, Jiao D, Sun Z, Wu K, Zhao Y, Han X. TTN/OBSCN 'Double-Hit' predicts favourable prognosis, 'immune-hot' subtype and potentially better immunotherapeutic efficacy in colorectal cancer. *J Cell Mol Med*. 2021;25(7):3239–3251. <https://doi.org/10.1111/jcmm.16393>. Epub 2021 Feb 23. PMID: 33624434; PMCID.
 42. Tsui YM, Chan LK, Ng IOL. Cancer stemness in hepatocellular carcinoma: mechanisms and translational potential. *Br J Cancer*. 2020;122:1428–40. <https://doi.org/10.1038/s41416-020-0823-9>.
 43. Seaby EG, Pengelly RJ, Ennis S. Exome sequencing explained: a practical guide to its clinical application. *Brief Funct Genomics*. 2016;15(5):374–84. <https://doi.org/10.1093/bfgp/evl054>.
 44. Feng W, Zhao S, Xue D, et al. Improving alignment accuracy on homopolymer regions for semiconductor-based sequencing technologies. *BMC Genomics*. 2016;17(Suppl 7):521. <https://doi.org/10.1186/s12864-016-2894-9>.
 45. Javanmard D, Najafi M, Babaei MR, et al. Investigation of CTNNB1 gene mutations and expression in hepatocellular carcinoma and cirrhosis in association with hepatitis B virus infection. *Infect Agents Cancer*. 2020;15:37. <https://doi.org/10.1186/s13027-020-00297-5>.
 46. Shibata, T. Genomic landscape of hepatocarcinogenesis. *J Hum Genet*. 2021;66:845–51. <https://doi.org/10.1038/s10038-021-00928-8>.
 47. Liang N, Yang T, Huang Q, et al. Mechanism of cancer stemness maintenance in human liver cancer. *Cell Death Dis*. 2022;13:394. <https://doi.org/10.1038/s41419-022-04848-z>.
 48. Zhu X, Wang Z, Qiu X, Wang W, Bei C, Tan C, Qin L, Ren Y, Tan S. Rs2303428 of MSH2 is associated with hepatocellular carcinoma prognosis in a chinese population. *DNA Cell Biol*. 2018;37(7):634–641. <https://doi.org/10.1089/dna.2018.4224>. Epub 2018 Jun 6. PMID: 29874113.
 49. Geramoutsou C, Nikou S, Karavias D, Arbi M, Tavlas P, Tzelepi V, Lygerou Z, Maroulis I, Bravou V. (2022): Focal adhesion proteins in hepatocellular carcinoma: RSU1 a novel tumour suppressor with prognostic significance. *Pathol Res Pract*. 2022;235:153950. <https://doi.org/10.1016/j.prp.2022.153950>. Epub 2022 May 23 PMID: 35642986.
 50. Hernández-Oliveras A, Izquierdo-Torres E, Hernández-Martínez G, Zarain-Herzberg Á, Santiago-García J. Transcriptional and epigenetic landscape of Ca²⁺-signaling genes in hepatocellular carcinoma. *J Cell Commun Signal*. 2021;15(3):433–445. <https://doi.org/10.1007/s12079-020-00597-w>. Epub 2021 Jan 4. PMID: 33398721; PMCID: PMC8222487.
 51. Sun EJ, Wankell M, Palamuthusingam P, McFarlane C, Hebbard L. Targeting the PI3K/Akt/mTOR pathway in hepatocellular carcinoma. *Biomedicines*. 2021;9:1639. <https://doi.org/10.3390/biomedicines9111639>.
 52. Farzaneh Z, Vosough M, Agarwal T, et al. Critical signaling pathways governing hepatocellular carcinoma behavior; small molecule-based approaches. *Cancer Cell Int*. 2021;21:208. <https://doi.org/10.1186/s12935-021-01924-w>.
 53. Zhang Y, Wang X. Targeting the Wnt/β-catenin signaling pathway in cancer. *J Hematol Oncol*. 2020;13:165. <https://doi.org/10.1186/s13045-020-00990-3>.
 54. Liu Y, Wang X, Yang Y. Hepatic Hippo signaling inhibits development of hepatocellular carcinoma. *Clin Mol Hepatol*. 2020;26(4):742–50. <https://doi.org/10.3350/cmh.2020.0178>. PMID: 32981290; PMCID: PMC7641559.
 55. Shi H, Zou Y, Zhong W, et al. Complex roles of Hippo-YAP/TAZ signaling in hepatocellular carcinoma. *J Cancer Res Clin Oncol*. 2023;149:15311–22. <https://doi.org/10.1007/s00432-023-05272-2>.
 56. Gao L, Zhang Z, Zhang P, Yu M, Yang T. Role of canonical Hedgehog signaling pathway in liver. *Int J Biol Sci*. 2018;14(12):1636. <https://doi.org/10.7150/ijbs.28089>. PMID: 30416378; PMCID: PMC6216024.
 57. Moon H, Ro SW. MAPK/ERK signaling pathway in hepatocellular carcinoma. *Cancers (Basel)*. 2021;13(12):3026. <https://doi.org/10.3390/cancers13123026>. PMID: 34204242; PMCID: PMC8234271.
 58. Nicholas TJ, Cormier MJ, Huang X, Qiao Y, Marth GT, Quinlan AR. OncoGEMINI: software for investigating tumor variants from multiple biopsies with integrated cancer annotations. *Genome Med*. 2021;13(1):46. <https://doi.org/10.1186/s13073-021-00854-6>. PMID: 33771218; PMCID: PMC7995589.

Publisher's Note

Springer Nature remains neutral with regard to jurisdictional claims in published maps and institutional affiliations.